Research Square

Preprints are preliminary reports that have not undergone peer review.
They should not be considered conclusive, used to inform clinical practice,
or referenced by the media as validated information.

A Tropical–Extratropical Connection Between the Intertropical Convergence Zone and Mediterranean Hydroclimate Variability

tamar eshet

tamar.eshet@mail.huji.ac.il

Hebrew University of Jerusalem

Sigalit Berkovic

Israel Institute for Biological Research

Assaf Hochman

Hebrew University of Jerusalem

Article

Keywords: Hadley cell, Extreme precipitation, ITCZ, Subseasonal-to-seasonal predictability, Middle East, Mediterranean cyclones, Moisture transport

Posted Date: November 4th, 2026

DOI: https://doi.org/10.21203/rs.3.rs-11349505/v1

License: This work is licensed under a Creative Commons Attribution 4.0 International License.
Read Full License

Additional Declarations: No competing interests reported.

A Tropical–Extratropical Connection Between the Intertropical Convergence Zone and Mediterranean Hydroclimate Variability

Tamar Eshet[1, *], Sigalit Berkovic[2], Assaf Hochman[1, *]

1. Fredy and Nadine Herrmann, Institute of Earth Sciences, The Hebrew University of Jerusalem, Israel.

2. Department of Applied Mathematics, IIBR, Ness-Ziona, Israel.

*Correspondence to: tamar.eshet@mail.huji.ac.il; Assaf.Hochman@mail.huji.ac.il

Abstract

The Mediterranean climate emerges from complex interactions between tropical and extratropical systems, yet the extent to which tropical variability, particularly that of the Intertropical Convergence Zone (ITCZ), links to Mediterranean hydroclimate remains poorly understood. Here, we show that interannual variability in ITCZ latitude, expansion, and intensity strongly and heterogeneously links with autumn (SON) precipitation across the Mediterranean Basin, revealing a previously underappreciated coupling between the tropics and extratropics. Using ERA5 reanalysis (1940–2024), we find that northward or expanded ITCZ states are linked to enhanced rainfall in the western (~+20 mm/season) and eastern (~+50 mm/season) Mediterranean. In contrast, an intensified ITCZ, marked by stronger deep convection in the tropics, is linked to suppressed rainfall in these regions (~ -20 to -50 mm/season) but increased rainfall over southern central Europe (~+100 mm/season).

By ranking years by each ITCZ attribute and compositing the top and bottom 20% of seasons, we isolate the distinct atmospheric circulation patterns associated with each ITCZ variability mode. The results indicate coherent responses in integrated water-vapor fluxes, cyclone track density, and Hadley-cell overturning, which together shape regional precipitation anomalies. Enhanced moisture transport accompanies northward ITCZ displacements in the west, while increased cyclone activity drives wetter conditions in the east. Conversely, high-intensity ITCZ phases coincide with reduced cyclone density and drying over the central Mediterranean. Notably, mid-tropospheric zonal circulation shows no significant variation except in small regions of the eastern Mediterranean, suggesting that tropical links to Mediterranean rainfall may operate primarily through meridional adjustments rather than zonal shifts. Stream-function

diagnostics further reveal significant differences confined to the western Mediterranean, where northward ITCZ displacements strengthen vertical ascent between ~25° and 35° N, linking tropical convection to mid-latitude precipitation.

Together, these results suggest that ITCZ variability is a potentially important yet underexplored correlate of Mediterranean hydroclimate variability, highlighting tropical–extratropical connections that warrant further investigation for their relevance to seasonal prediction and climate projections.

Keywords: Hadley cell; Extreme precipitation; ITCZ; Subseasonal-to-seasonal predictability; Middle East; Mediterranean cyclones; Moisture transport

1. Introduction

The Mediterranean basin is a global climate "hotspot," where small shifts in atmospheric circulation can yield disproportionately large impacts on precipitation, ecosystems, and human activity [1–3]. Autumn precipitation is a key contributor to regional water resources, yet it shows pronounced interannual variability driven by a complex interplay between tropical and extratropical processes. Understanding the large-scale drivers of this variability is essential for improving predictions of hydroclimate extremes, which are expected to intensify due to ongoing climate change [4, 5].

Much of the existing literature attributes Mediterranean rainfall variability to midlatitude and regional circulation modes such as the North Atlantic Oscillation (NAO), the East Atlantic Pattern, and variations in Mediterranean cyclone activity[6–12]. These patterns modulate storm tracks, air–sea exchanges, and moisture advection but fail to fully explain the amplitude and spatial asymmetry of rainfall variability, particularly during the transition seasons.

Increasing evidence indicates that tropical processes also play an essential role in shaping Mediterranean hydroclimate[13–16]. Two well-established pathways are moisture transport from the tropics into the Mediterranean via tropical plumes and atmospheric rivers[17]. These mechanisms often coexist, with tropical plumes providing a morphological manifestation of tropical moisture export and atmospheric rivers quantifying the associated moisture transport. When such moisture-rich intrusions interact with upper-level troughs, cut-off lows, or Mediterranean cyclones, they can

63 substantially enhance precipitation and contribute to extreme rainfall events,
64 particularly during autumn and early winter.[13,18–25].

65 The Mediterranean is also partially integrated into Africa's tropical circulation through
66 thermally driven pressure contrasts. The Mediterranean Pressure Index (MPI), defined
67 as the sea-level pressure difference between the northern and southern basins, is
68 anticorrelated with the Indian Monsoon Index, with maximum correlation in late
69 summer and autumn[26]. The MPI reflects the geostrophic and meridional wind
70 components that govern inflow into the African Intertropical Convergence Zone
71 (ITCZ), illustrating a physical linkage between Mediterranean and tropical pressure
72 systems. In addition, a northward shift of the Hadley cell lowers surface pressure over
73 the Mediterranean and increases the frequency of cyclones and precipitation[27].

74 Moreover, the influence of tropical modes such as the El Niño-Southern Oscillation
75 (ENSO) and the Indian Ocean Dipole (IOD) on Mediterranean rainfall is strongest in
76 October [4,28], coinciding with the maximum correlation between the MPI and the Indian
77 monsoon[26]. Large-scale upper-tropospheric patterns, including blocking and split-flow
78 configurations over northern Europe, further shape Mediterranean precipitation
79 variability during this season[29,30].

80 Other tropical-origin circulation systems, such as the Red Sea Trough, also modulate
81 rainfall in the eastern Mediterranean. Originating from the Sudan Monsoon Low, the
82 Red Sea Trough represents a subtropical–equatorial thermal low that can generate either
83 wet or dry anomalies depending on its intensity and orientation[31–35]. These systems
84 emphasize the Mediterranean's sensitivity to tropical–subtropical linking.

85 Despite these established connections, the direct role of the ITCZ, the planet's primary
86 convective and energy-transfer system, remains largely unexplored in the context of
87 Mediterranean hydroclimate. The ITCZ organizes global deep convection and latent
88 heat release, shaping the position of the Hadley cell and influencing cross-equatorial
89 energy and moisture transport[36,37]. Variability in ITCZ latitude, expansion, and
90 intensity has been demonstrated to impact tropical and subtropical precipitation, with
91 teleconnections extending into the midlatitudes[38,39]. The ITCZ shifts meridionally on
92 seasonal to interannual timescales, migrating by several degrees of latitude annually
93 and exhibiting shorter-term excursions linked to oceanic and radiative forcing such as
94 ENSO, volcanic activity, and solar variability[37,40]. Over the Atlantic, ITCZ migration

is primarily controlled by cross-equatorial energy fluxes, while in the Pacific and Indian basins it is dominated by internal ocean–atmosphere variability[41]. Even small shifts in ITCZ latitude can substantially alter precipitation and convection near its boundaries, affecting adjacent subtropical regions such as North Africa and the Mediterranean.

The Mediterranean's position at the northern edge of the Hadley cell makes it particularly sensitive to these tropical displacements. During autumn (September - November), this sensitivity peaks as the ITCZ retreats equatorward while the Mediterranean enters its active cyclonic season. Autumn also marks the period of most frequent extreme precipitation events[18,30], when elevated sea-surface temperatures contrast with rapidly cooling continental surfaces, increasing baroclinicity and favoring deep convection[42,43].

North Africa lies at the poleward boundary of the ITCZ, and northward ITCZ shifts have been associated with enhanced rainfall and the historical expansion of lakes and rivers in the region[44]. Similar displacements have been linked to heavy rain over southern Iran and the Arabian Peninsula, where intensified Sudanese low-pressure systems extend tropical convection northward into the eastern Mediterranean, often triggering flash floods[45,46].

Given this convergence of dynamical processes, autumn provides an ideal natural laboratory for studying how tropical variability, particularly the ITCZ, correlates with Mediterranean rainfall. Yet, despite the strong physical basis for this connection, no systematic assessment has quantified how interannual ITCZ variability links to Mediterranean hydroclimatic conditions.

This study addresses that gap by examining the relationship between ITCZ variability and Mediterranean autumn precipitation using dynamical and thermodynamical diagnostics. We characterize ITCZ variability through three complementary metrics - latitude, latitudinal extent (expansion), and intensity - derived from outgoing longwave radiation (OLR) using a threshold of 240 W m^{-2} [47–49]. To resolve longitudinal differences in ITCZ–rainfall associations, we calculate these metrics separately within three 20°-wide longitude bands corresponding broadly to the western, central, and eastern Mediterranean sectors (Fig. 1). This subdivision follows the general regional approach of Giorgi and Lionello (2008) [2], with boundaries adapted for this study. Sensitivity tests show no substantial changes in results when we vary the longitude

bands. Using ERA5[50] reanalysis and CRU [51] observational data for 1940–2024, we assess associations between these ITCZ metrics and autumn precipitation within the corresponding Mediterranean sectors (Fig. 1; Sect. 2.1). To investigate potential physical mechanisms underlying these associations (Sect. 2.2), we examine four complementary diagnostics: (1) vertically integrated water-vapor transport (IVT), characterizing large-scale moisture flux; (2) geopotential height at 500 hPa (Z500), describing mid-tropospheric circulation; (3) cyclone track density derived from the confidence-level-5 tracks in the composite dataset of Flaounas et al. (2023) [1], used to quantify synoptic activity; and (4) the meridional mass stream function, characterizing variations in the Hadley circulation.

By disentangling these processes, this work aims to establish whether the ITCZ may serve as a dynamic atmospheric bridge linking tropical convection to Mediterranean precipitation variability. Clarifying this connection advances our understanding of tropical–extratropical interactions, may provide a physical basis for improved seasonal predictability, and may offer a framework for assessing how projected ITCZ shifts under climate change may reshape precipitation patterns in one of the world's most climate-sensitive regions.

2. Results

2.1. Observed correlations between ITCZ variability and Mediterranean precipitation

The correlation between autumn (SON) Mediterranean precipitation and the ITCZ's latitude, expansion, and intensity shows clear, regionally organized patterns across the basin (Figs. 1-4). The Spearman correlations indicate that precipitation variability in the western and eastern Mediterranean is most strongly linked to the ITCZ latitude and expansion (Fig. 2a, c, d, f). In contrast, the central basin exhibits weaker or opposite relationships (Fig. 2b, e, h).

Periods characterized by a northward or broadened ITCZ correspond to enhanced rainfall in the western and eastern Mediterranean ($r \approx 0.4$), with positive correlations extending across Morocco, southern Spain, Algeria, Tunisia, the Balkans, and the Levant (Fig. 2a-f, $r \approx 0.3$). These patterns may indicate that meridional shifts and widening of the tropical convective belt may partly enhance poleward moisture delivery into both ends of the basin. Conversely, ITCZ intensity**,** representing the strength of

tropical convection, exhibits a negative correlation with precipitation over the same regions (Fig. 2g, i; $r \approx -0.4$) but a positive correlation over southern central Europe, pronounced over Italy, the Adriatic Sea, Greece, and Yugoslavia (Fig. 2h; $r \approx 0.4$). This inverse relationship may suggest that strong tropical convection may suppresse rainfall over the subtropical Mediterranean while favoring precipitation farther north. The correlation structures are robust across datasets: the Climate Research Unit (CRU) [51] observational precipitation dataset yields nearly identical spatial patterns, confirming ERA5's reliability in capturing interannual hydroclimatic variability (Fig. S1).

The ITCZ attributes themselves are also interrelated (Fig. 3). Latitude and expansion are positively correlated in the western ($r=0.68$, $R^2=0.46$) and eastern Mediterranean ($r=0.77$, $R^2=0.59$), reflecting the tendency for poleward ITCZ displacements to coincide with broader convective zones (Fig. 3a, c). This suggests that ITCZ broadening occurs predominantly through poleward expansion. In contrast, intensity is negatively correlated with expansion in the western ($r=-0.89$, $R^2=0.80$) and the eastern Mediterranean ($r=-0.70$, $R^2=0.49$; Fig. 3g, i), consistent with the well-documented "width–strength trade-off" in tropical dynamics [38,52]

To isolate the independent contribution of each ITCZ attribute, partial correlations were computed while controlling for the other two (Fig. 4). The analysis reveals distinct regional signatures: latitude exerts the strongest significant positive correlation with precipitation in western France, south England, northwestern Africa (Fig. 4a), Algeria, and Tunisia (Fig. 4b)**.** Expansion dominates over eastern Europe (Romania, Ukraine, West Russia; Fig. 4f)**,** and intensity produces a meridional dipole with significant negative correlations over North Africa and the eastern Mediterranean, and significant positive correlations across southern central Europe (Fig. 3h, i). These correlations remain robust when using observational precipitation, underscoring their statistical significance (Fig. S2).

Composite analyses of the top and bottom 20% of ITCZ years further illustrate the regional expression of these links, presenting 8 years for each extreme season (Fig. 5). During northward-shifted and expanded ITCZ years, precipitation anomalies are markedly positive in the western and eastern Mediterranean, while the central basin experiences weak or negative anomalies (Fig. 5a-f). In contrast, intense ITCZ years correspond to wetter conditions along the Mediterranean margins and decreased rainfall over southern central Europe (Fig. 5g-i).

Although regional correlations indicate a negative association between ITCZ intensity and precipitation in the eastern and western Mediterranean (Figs. 2g–i and 4g–i), the composites reveal a more spatially heterogeneous pattern, with localized positive anomalies within the basin alongside pronounced drying over southern–central Europe (Fig. 5g–i). This contrast may reflect differences in spatial aggregation and sampling: correlations summarize linear associations across the full range of ITCZ variability, whereas composites characterize spatial precipitation patterns during selected extreme ITCZ states. The broader negative association may be consistent with a link between tropical heating and enhanced Mediterranean subsidence, analogous to the summer monsoon–desert mechanism described by Rodwell and Hoskins (1996) [16], although its relevance to autumn requires further investigation. Shifts in moisture transport or storm tracks during extreme ITCZ states may also favor localized rainfall increases even where the broader regional association is negative (Sect. 2.2). These contrasting patterns highlight the regional specificity of ITCZ–precipitation relationships, although they do not, by themselves, establish nonlinearity.

Overall, northward ITCZ displacement and greater latitudinal extent are generally associated with enhanced Mediterranean rainfall, whereas greater ITCZ intensity is associated with reduced rainfall, with substantial spatial variation. Together, these findings suggest a previously underexplored connection between tropical variability and Mediterranean autumn hydroclimate.

2.2. Mechanisms linking ITCZ variability to Mediterranean hydroclimate

We explore the processes underlying the observed correlations by analyzing large-scale moisture flux (Fig. 6)**,** synoptic cyclone activity (Figs. 7-9), and meridional overturning circulation (Figs. 10-12). Together, these diagnostics show that the ITCZ correlates with Mediterranean precipitation primarily through meridional mechanisms, rather than through changes in mid-tropospheric zonal circulation. The IVT composites (Fig. 6) indicate that moisture flux plays a central role in mediating the ITCZ's link to the Mediterranean. During northward ITCZ years, poleward moisture fluxes strengthened across northern Africa and the western Mediterranean**,** consistent with an increased inflow of humid air (Fig. 6a). The expanded ITCZ states reduce moisture flux over the central Mediterranean, producing widespread negative flux anomalies (Fig. 6e). In contrast, intense ITCZ years exhibit a pronounced meridional gradient, with reduced IVT across North Africa and southern Europe, matching the observed drying (Fig. 6g-

i). These results indicate that the ITCZ latitude and width primarily modulate precipitation by altering moisture availability and advection pathways. At the same time, intensity affects vertical transport efficiency by modifying convection and subsidence.

Variations in Mediterranean cyclone activity provide a complementary synoptic-scale mechanism (Figs. 7-9). In northward ITCZ years**,** cyclone track density increases over the eastern Mediterranean, particularly around Cyprus and the Levant, while decreasing over the Black Sea, implying a southward shift in synoptic activity that enhances rainfall in the eastern basin (Fig. 7c, f, i). Under expanded ITCZ conditions, cyclone track density decreases across southern central Europe (Fig. 8b, e, h), consistent with drier conditions over Italy (Fig. 5e). During intense ITCZ years, cyclone tracks are significantly reduced in the central Mediterranean (Fig. 9b, e, h), coinciding with suppressed precipitation (Fig. 5h). These results suggest that ITCZ-driven changes in tropical convection correlate with the frequency and positioning of Mediterranean cyclones, thereby modulating seasonal rainfall.

To assess the interaction between tropical convection and Mediterranean vertical motion, we analyzed the mass stream function associated with the Hadley circulation (Figs. 10-12). During northward ITCZ phases, the ascending branch of the Hadley cell intensifies between 25°N and 35°N, centered over the western Mediterranean (Fig. 10a, d, g), coinciding with the region of maximum precipitation response (Fig. 5a). This strengthened ascent likely enhances convective instability and vertical moisture fluxes. During expanded ITCZ states, ascent intensifies near 30°N, accompanied by compensating descent farther north, producing a meridional dipole structure (Fig. 11a, d, g). This is consistent with increased rainfall around 30°N and reduced precipitation over northern Europe (Fig. 5d-f). In contrast, high-intensity ITCZ years show weaker, spatially confined anomalies, with significant differences restricted to the western Mediterranean (Fig. 12a, d, g). The eastern basin exhibits limited stream-function responses (Fig. 10-12c, f, i) despite significant rainfall anomalies (Fig. 5c, f, i), suggesting that local processes, particularly cyclone modulation and moisture redistribution, dominate in this region (Fig. 7c, f, i and Fig. 6c, f, i).

Composite differences in Z500 between the upper and lower 20% of seasons show no robust signal over the Mediterranean, except for a weak response to ITCZ intensity in the eastern Mediterranean. This indicates that the ITCZ–Mediterranean connection is

largely mediated not by large-scale zonal flow or planetary-wave adjustments (Fig. S3), but by changes in meridional circulation, vertical motion, and moisture flux over the western Mediterranean.

Overall, the results show that interannual shifts in the ITCZ's latitude, expansion, and intensity leave a dynamical imprint on Mediterranean autumn precipitation. Variations in meridional moisture flux, cyclone frequency, and Hadley circulation confirm the ITCZ as a key bridge linking tropical convection to subtropical hydroclimate. The lack of zonal-circulation anomalies suggests this connection acts primarily through vertical and meridional processes (see Table 1 for a summary of main findings). These results form the basis for the following discussion on tropical–extratropical linkages, regional predictability, and the ITCZ's sensitivity to climate changes.

3. Discussion and Conclusions

Our results identify a previously underexplored association between interannual ITCZ variability and Mediterranean autumn precipitation. Previous studies have established the importance of large-scale circulation patterns, including the North Atlantic Oscillation (NAO), for Mediterranean rainfall variability [7,53,54]. The present analysis complements this understanding by showing that ITCZ latitude, expansion, and intensity are associated with distinct regional precipitation patterns. Northward displacement and greater latitudinal extent generally coincide with wetter conditions in the western and eastern Mediterranean, whereas greater intensity is associated with reduced rainfall in these regions and increased precipitation over southern–central Europe. These relationships suggest that distinguishing between ITCZ position, extent, and convective intensity is important for characterizing its connections with Mediterranean hydroclimate.

The composite diagnostics provide a physical context for these associations. Northward ITCZ displacements and greater expansion coincide with enhanced moisture flux into the western Mediterranean, consistent with the role of tropical moisture transport in supplying extratropical precipitation [55]. The stream function composites also indicate enhanced ascent between approximately 25° and 35° N in the western sector during northward ITCZ states. Together, these anomalies suggest that moisture availability and regional overturning may contribute to the western Mediterranean rainfall signal. In the eastern Mediterranean, increased cyclone track density accompanies wetter conditions,

while vertical-circulation anomalies associated with ITCZ latitude and expansion are weaker or statistically insignificant. This contrast suggests a greater contribution from synoptic activity in the east, consistent with the importance of cyclones for regional precipitation[1]. Related connections between tropical variability, moisture transport, and Cyprus Low occurrence have been documented for ENSO and the Indian Ocean Dipole (IOD)[4], although those findings do not establish an equivalent pathway for ITCZ variability.

ITCZ intensity exhibits a different set of associations. High-intensity seasons coincide with weaker cyclone activity and drying over parts of the Mediterranean, alongside significant vertical-mass-transport anomalies in the central and eastern sectors. One possible interpretation is that stronger tropical convective heating accompanies changes in subtropical overturning that favor regional subsidence and atmospheric stability. Such a pathway is physically plausible in light of the summer monsoon–desert mechanism described by Rodwell and Hoskins (1996) [16], but its applicability to autumn requires further investigation. The contrasting rainfall association over southern–central Europe further indicates that stronger tropical convection is not accompanied by uniform drying across the wider region. Establishing whether this spatial contrast reflects changes in moisture convergence, cyclone pathways, or vertical motion would require a more explicit assessment of their respective contributions.

The regional correlations and extreme-state composites offer complementary perspectives on these relationships. Correlations summarize linear associations across the full range of ITCZ variability, whereas composites emphasize precipitation and circulation patterns during the upper and lower quantiles of ITCZ states. Localized wet anomalies can therefore coexist with negative regional correlations [56]. The broad agreement between these analyses, together with the insensitivity of the main findings to the choice of longitude bands, supports the robustness of the identified associations.

To assess potential overlap with established climate modes, we examined correlations between the ITCZ metrics and the NAO, ENSO, and IOD indices. We found no statistically significant relationships except a weak significant association between ENSO and ITCZ latitude in the western Mediterranean ($r = 0.29$) and ITCZ expansion in the Eastern Mediterranean ($r = 0.28$). This finding suggests that the ITCZ metrics do not simply reproduce the contemporaneous linear variability of these indices, although it does not exclude lagged relationships, nonlinear dependencies, or shared forcing.

Likewise, the limited Z500 anomalies - apart from a small decrease over the eastern Mediterranean in the intensity composites - provide little evidence for a coherent mid-tropospheric wave-train pattern. They do not, however, rule out changes in upper-level circulation or jet position. Because this study is based on monthly temporal resolution, it cannot fully resolve variability on synoptic timescales and therefore, conclusions regarding changes in synoptic-scale systems are necessarily limited. The moisture-flux, cyclone, and stream function diagnostics should therefore be interpreted as evidence for plausible contributing processes rather than proof of a uniquely meridional or causal pathway.

These findings motivate an assessment of whether ITCZ metrics provide additional information for predicting Mediterranean autumn rainfall. Forecast and reforecast archives, such as those assembled through the Subseasonal to Seasonal Prediction Project [57], offer a framework for evaluating the predictability of the metrics and their relationships with regional precipitation. Any practical benefit would need to be demonstrated through out-of-sample tests against forecasts based on established predictors. In particular, contemporaneous associations alone do not establish useful forecast lead times or improved skill in predicting droughts and floods.

The implications for climate change also require caution. Projected changes in ITCZ location, width, and strength depend on the region, season, diagnostic, and forcing, rather than following a uniform poleward shift and intensification [52]. Moreover, historical interannual relationships need not remain unchanged under sustained warming. The associations identified here therefore provide a basis for testing how climate models represent tropical–Mediterranean connections, rather than directly predicting future regional rainfall changes. Evaluating both the ITCZ metrics and their accompanying moisture-transport and circulation patterns could help determine whether these relationships persist across climate states.

Overall, this study identifies a robust but spatially heterogeneous connection between ITCZ variability and Mediterranean autumn precipitation. Its main contribution is to distinguish the rainfall associations of ITCZ position and extent from those of convective intensity, and to identify accompanying moisture-transport, cyclone, and vertical-circulation anomalies. These results broaden the physical context for understanding Mediterranean hydroclimate variability and provide testable hypotheses for future process-based and prediction studies.

4. Data and Methods

4.1. Data

The ITCZ is a climatological band of enhanced convection rather than a coherent synoptic-scale feature; its metrics are typically studied using monthly mean statistics [39,58]. To examine the relationship between ITCZ characteristics and Mediterranean precipitation during autumn (September-November), we used monthly data from the ERA5 reanalysis, produced by the European Centre for Medium-Range Weather Forecasting [50]. The ERA5 dataset provides continuous, global coverage of atmospheric, land-surface, and oceanic variables at a 0.25° × 0.25° grid spacing. Because reanalysis precipitation fields are generated through model forecasts that assimilate background fields and omit rain gauge data[59]; we assessed the reliability of ERA5 precipitation by comparing it with the Climatic Research Unit (CRU) observational dataset, which combines weather station, satellite, and ancillary sources at a 0.5° × 0.5° grid spacing [51]. To allow meaningful comparisons across regions with different climatological rainfall regimes, we present precipitation anomalies in units of local standard deviation, calculated at each grid point.

The Mediterranean domain was defined as 20°W–40°E and 25°N –55°N (Fig. 1). We analyzed the period from 1940 to 2024, including Outgoing Longwave Radiation (OLR) for ITCZ identification at longitudes between 20°S-30°N (Fig. 1), and total precipitation for hydroclimatic assessment. To characterize large-scale atmospheric circulation, we used 500-hPa geopotential height (Z500). We also diagnosed the Hadley circulation using the zonal-mean Eulerian mass stream function, computed from the meridional wind (v) at 1000-200 hPa.

We characterized atmospheric moisture transport using the monthly mean eastward and northward vertically integrated water-vapor flux components provided by ERA5. These components represent moisture transport integrated over the full atmospheric column and are defined as:

$$\overline{Q_x} = \frac{1}{g}\overline{\int_{p_{top}}^{p_s} qu\, dp}$$

$$\overline{Q_y} = \frac{1}{g}\overline{\int_{p_{top}}^{p_s} qv\, dp}$$

Here, q is specific humidity, u and v are the zonal and meridional wind components, g is gravitational acceleration, and the integration extends from the top of the atmosphere to surface pressure p_s, with pressure expressed in Pa. Overbars denote monthly averaging. We calculate the magnitude of the monthly mean integrated transport as:

$$IVT = \sqrt{\overline{Q_x}^2 + \overline{Q_y}^2}$$

IVT is expressed in kg m^{-1} s^{-1}. This quantity describes the magnitude of the monthly mean moisture-transport vector, rather than the monthly average of instantaneous IVT magnitude.

4.2. Characterization of ITCZ variability

To identify the ITCZ, we used OLR as a key diagnostic variable, since regions of low OLR reliably indicate deep convective activity characteristic of the ITCZ[37,47,48]. This approach clearly delineates the ITCZ's position and seasonal migration. Many studies have characterized the ITCZ as a zone of maximum cloudiness and precipitation, readily observable in satellite-derived OLR measurements[47–49]. OLR data provide consistent spatial coverage. It circumvents the limitations of spatial inhomogeneity in station-based rainfall records, thereby enabling robust quantification of the ITCZ's spatiotemporal evolution[47]. Before analysis, we applied grid-point linear least-squares detrending to remove long-term climate trends. For the study domain, we used an OLR threshold of 240 W m^{-2} to delineate the ITCZ region, capturing both moderate and strong convective activity associated with the ITCZ over Africa[47–49].

We analysed three ITCZ characteristics: latitude, expansion, and intensity. Latitude was defined as the monthly mean position of the northern ITCZ boundary, expansion as the monthly mean latitudinal distance between its northern and southern boundaries, and intensity as the monthly mean OLR within the ITCZ area, with lower OLR indicating stronger convection. To characterize longitudinal differences in ITCZ–Mediterranean precipitation associations, we calculated these metrics separately within three 20°-wide sectors: western (20°W–0°), central (0°–20°E), and eastern (20°E–40°E; Fig. 1). This width provides a practical balance between averaging over small-scale longitudinal variability and retaining regional contrasts that could be obscured by averaging across the entire domain. The sectors represent geographical averaging domains rather than closed circulation cells or prescribed moisture-transport pathways. Although the

Coriolis force deflects poleward flow eastward in the Northern Hemisphere, this does not preclude examining statistical associations within corresponding longitude bands: regional overturning and moisture transport can include both meridional and zonal components and extend across sector boundaries [60]. The 20° width is therefore a methodological choice rather than a dynamically prescribed scale. Sensitivity tests using alternative longitude bands produced no substantial changes in the main results, supporting its suitability for characterizing the regional associations examined here.

We ranked years by each ITCZ characteristic and selected the upper and lower 20% to represent contrasting ITCZ cases while maintaining a sufficient sample size for statistical robustness. We composited large-scale atmospheric variables for these distinct years to examine associated circulation patterns. To assess statistical significance, we applied a two-sided Student's t-test at the 90% significance level to geopotential height, which approximately follows a normal distribution. In contrast, we used a bootstrap resampling procedure with 1000 iterations for the remaining variables that did not meet normality assumptions. Given the smaller sample size in the extreme-season analysis, we adopted a 90% significance level to account for reduced statistical power.

To investigate the statistical relationships between ITCZ characteristics and Mediterranean precipitation, we employed Spearman's rank correlation, a nonparametric alternative to Pearson's correlation that measures the strength of monotonic associations based on ranked values[61]. We also conducted a partial correlation analysis to isolate each ITCZ attribute's contribution while controlling for the other two, using linear regression to remove interdependencies.

4.3 Mediterranean cyclone tracking

To assess the link between ITCZ variability and Mediterranean precipitation through cyclone track density, we analyzed composite Mediterranean cyclone tracks from Flaounas et al. (2023)[1]. Cyclone detection and tracking methods (CTDMs) vary significantly in their algorithms and physical assumptions, leading to discrepancies in the cyclone characteristics they identify. Many CTDMs tend to generate an excessive number of weak or short-lived features that do not correspond to genuine large-scale or mesoscale cyclones[1,62].

To address these inconsistencies, Flaounas et al. (2023) [1] developed a composite Mediterranean cyclone track dataset that integrates outputs from ten independent, well-established CTDMs. Each composite track is assigned a confidence level ranging from 2 to 10, corresponding to the number of CTDMs that identified the same cyclone. Following the authors' recommendation, we used tracks with a confidence level of five to balance statistical robustness with consistency with expert cyclone identification.

4.4 Diagnosing Hadley cell variability

To assess the meridional circulation patterns associated with ITCZ variability, we computed the mass stream function from ERA5 meridional wind (v) data over 10°S–50°N, following Lachmy and Kaspi (2020)[63], which defined it as:

$$\Psi(\phi, p) = \frac{2\pi a cos\phi}{g} \int \bar{v}^{lon}(\phi, p) dp$$

Here, ψ is the zonal-mean meridional mass stream function, ϕ is latitude, p is pressure, a is Earth's radius, g is gravitational acceleration, and $\bar{v}^{lon}$ is the zonal-mean meridional wind. The integration is performed vertically in pressure from the top of the atmosphere to pressure level p. ψ is expressed in kg s^{-1} and describes the strength and direction of the meridional overturning circulation. The stream function diagnoses the mean meridional overturning circulation, capturing the Hadley cell and its shifts under different ITCZ conditions.

For the calculation, we averaged the v-wind over the central 5° of longitude in each Mediterranean sector to represent the zonal meridional flow in the western (12.5°W–7.5°W), central (7.5°E–12.5°E), and eastern (27.5°E–32.5°E) regions. This approach minimizes local disturbances while highlighting large-scale dynamical structures. Sensitivity tests with alternative configurations showed no significant impact on the results. We then used the resulting stream function to infer vertical velocity patterns, deriving the induced vertical and meridional motions (ω and υ) diagnostically from stream-function gradients and visualizing them as arrows to illustrate ascending and descending branches of the overturning circulation.

Acknowledgments

The Israel Science Foundation (grant #978/23), the NNRC of Israel, and the Planning and Budgeting Committee of the Israeli Council for Higher Education supported the contributions of TE and AH under the 'MedWORLD' Consortium.

Declaration of Generative AI and AI-assisted Technologies in the Writing Process

During the preparation of this work, the authors used ChatGPT and Grammarly to improve the language and readability. After using these tools, the authors reviewed and edited the article as needed and take full responsibility for the publication's content.

References

1. Flaounas, E. *et al.* A composite approach to produce reference datasets for extratropical cyclone tracks: application to Mediterranean cyclones. *Weather Clim. Dyn.* **4**, 639–661 (2023).
2. Giorgi, F. Climate change hot-spots. *Geophys. Res. Lett.* **33**, (2006).
3. Tuel, A. & Eltahir, E. A. Why is the Mediterranean a climate change hot spot? *J. Clim.* **33**, 5829–5843 (2020).
4. Hochman, A. & Gildor, H. Synergistic effects of El Niño–Southern Oscillation and the Indian Ocean Dipole on Middle Eastern subseasonal precipitation variability and predictability. *Q. J. R. Meteorol. Soc.* **151**, e4903 (2025).
5. Khodayar, S. *et al.* Mediterranean cyclones in a changing climate: A review on their socio-economic impacts. *Rev. Geophys.* **63**, e2024RG000853 (2025).
6. Hochman, A., Harpaz, T., Saaroni, H. & Alpert, P. Synoptic classification in 21st century CMIP5 predictions over the eastern Mediterranean with focus on cyclones. *Int. J. Climatol.* **38**, 1476–1483 (2018).
7. Trigo, R. M., Osborn, T. J. & Corte-Real, J. M. The North Atlantic Oscillation influence on Europe: climate impacts and associated physical mechanisms. *Clim. Res.* **20**, 9–17 (2002).
8. Ziv, B., Saaroni, H. & Alpert, P. The factors governing the interannual variability of rainfall over Israel. *Int. J. Climatol.* **26**, 55–69 (2006).
9. Hochman, A. *et al.* The dynamics of cyclones in the twenty-first century: The eastern Mediterranean as an example. *Clim. Dyn.* **54**, 561–574 (2020).

10. Reale, M., David, W., Narvaez, C., & others. Future projections of Mediterranean cyclone characteristics using the Med-CORDEX ensemble of coupled regional climate system models. *Clim. Dyn.* **58**, 2501–2524 (2022).
11. Reale, M. *et al.* Response of early winter precipitation and storm activity in the North Atlantic–European–Mediterranean region to Indian Ocean SST variability. *Geophys. Res. Lett.* **52**, e2025GL116732 (2025).
12. Sandler, D., Saaroni, H., Ziv, B., Tamarin-Brodsky, T. & Harnik, N. The connection between north Atlantic storm track regimes and eastern Mediterranean cyclonic activity. *Weather Clim. Dyn.* **5**, 1103–1116 (2024).
13. Krichak, S. O. *et al.* Discussing the role of tropical and subtropical moisture sources in cold season extreme precipitation events in the Mediterranean region from a climate change perspective. *Nat. Hazards Earth Syst. Sci.* **16**, 269–285 (2016).
14. Krichak, S. O., Breitgand, J. S., Gualdi, S. & Feldstein, S. B. Teleconnection–extreme precipitation relationships over the Mediterranean region. *Theor. Appl. Climatol.* **117**, 679–692 (2014).
15. Nicholson, S. E. The ITCZ and the seasonal cycle over equatorial Africa. *Bull. Am. Meteorol. Soc.* **99**, 337–348 (2018).
16. Rodwell, M. J. & Hoskins, B. J. Monsoons and the dynamics of deserts. *Q. J. R. Meteorol. Soc.* **122**, 1385–1404 (1996).
17. Spensberger, C., Konstali, K. & Spengler, T. Moisture transport axes: a unifying definition for tropical moisture exports, atmospheric rivers, and warm moist intrusions. *Weather Clim. Dyn.* **6**, 431–446 (2025).
18. Buzzi, A., Davolio, S., Malguzzi, P., Drofa, O. & Mastrangelo, D. Heavy rainfall episodes over Liguria in autumn 2011: numerical forecasting experiments. *Nat. Hazards Earth Syst. Sci.* **14**, 1325–1340 (2014).

19. Cloux, S., Garaboa-Paz, D., Insua-Costa, D., Miguez-Macho, G. & Pérez-Muñuzuri, V. Extreme precipitation events in the Mediterranean area: contrasting two different models for moisture source identification. *Hydrol. Earth Syst. Sci.* **25**, 6465–6477 (2021).
20. Davolio, S. *et al.* Detection of atmospheric rivers affecting the Mediterranean and producing extreme rainfall over northern-central Italy. *EGUsphere* **2025**, 1–19 (2025).
21. Dayan, U., Nissen, K. & Ulbrich, U. Atmospheric conditions inducing extreme precipitation over the eastern and western Mediterranean. *Nat. Hazards Earth Syst. Sci.* **15**, 2525–2544 (2015).
22. Fröhlich, L., Knippertz, P., Fink, A. H. & Hohberger, E. An objective climatology of tropical plumes. *J. Clim.* **26**, 5044–5060 (2013).
23. Insua-Costa, D., Miguez-Macho, G. & Llasat, M. C. Local and remote moisture sources for extreme precipitation: a study of the two catastrophic 1982 western Mediterranean episodes. *Hydrol. Earth Syst. Sci.* **23**, 3885–3900 (2019).
24. Tubi, A., Dayan, U. & Lensky, I. M. Moisture transport by tropical plumes over the Middle East: A 30-year climatology. *Q. J. R. Meteorol. Soc.* **143**, 3165–3176 (2017).
25. Tubi, A. & Dayan, U. Tropical Plumes over the Middle East: Climatology and synoptic conditions. *Atmos. Res.* **145–146**, 168–181 (2014).
26. Navarra, A. Teleconnections between Indian monsoon and Sahel rainfall and the Mediterranean. *Int. J. Climatol.* (2003).
27. Nojarov, P. The increase in September precipitation in the Mediterranean region as a result of changes in atmospheric circulation. *Meteorol. Atmos. Phys.* **129**, 145–156 (2017).

28. Hochman, A., Shachar, N. & Gildor, H. Unraveling Sub-Seasonal Precipitation Variability in the Middle East Via Indian Ocean Sea Surface Temperatures. *Sci. Rep.* **14**, 2919 (2024).
29. Sumner, E. A study of blocking in the Atlantic-European of the northern hemisphere. *Q. J. R. Meteorol. Soc.* **80**, 402–416 (1954).
30. Valero, F., Luna, M., Martín, M., Morata, A. & González-Rouco, F. Coupled modes of large-scale climatic variables and regional precipitation in the Western Mediterranean in autumn. *Clim. Dyn.* **22**, 307–323 (2004).
31. de Vries, A. J. Tropical-extratropical interactions and extreme precipitation events in the Middle East. (Johannes Gutenberg-Universität Mainz, 2018).
32. De Vries, A. J. *et al.* Identification of tropical-extratropical interactions and extreme precipitation events in the Middle East based on potential vorticity and moisture transport. *J. Geophys. Res. Atmos.* **123**, 861–881 (2018).
33. Hochman, A. *et al.* The sources of extreme precipitation predictability: the case of the `Wet' Red Sea Trough. *Weather Clim. Extrem.* **40**, 100564 (2023).
34. Hochman, A., Rostkier-Edelstein, D., Kunin, P. & Pinto, J. G. Changes in the characteristics of `wet' and `dry' Red Sea Trough over the Eastern Mediterranean in CMIP5 climate projections. *Theor. Appl. Climatol.* **143**, 781–794 (2021).
35. Tsvieli, Y. & Zangvil, A. Synoptic climatological analysis of'wet'and'dry'Red Sea Troughs over Israel. *Int. J. Climatol.* **25**, 1997–2016 (2005).
36. Donohoe, A., Marshall, J., Ferreira, D. & Mcgee, D. The relationship between ITCZ location and cross-equatorial atmospheric heat transport: From the seasonal cycle to the Last Glacial Maximum. *J. Clim.* **26**, 3597–3618 (2013).
37. Waliser, D. E. & Gautier, C. A satellite-derived climatology of the ITCZ. *J. Clim.* **6**, 2162–2174 (1993).

38. Adam, O. Dynamic and energetic constraints on the modality and position of the intertropical convergence zone in an aquaplanet. *J. Clim.* **34**, 527–543 (2021).
39. Byrne, M. P. & Schneider, T. Energetic constraints on the width of the intertropical convergence zone. *J. Clim.* **29**, 4709–4721 (2016).
40. Bischoff, T. & Schneider, T. Energetic constraints on the position of the intertropical convergence zone. *J. Clim.* **27**, 4937–4951 (2014).
41. Roldán-Gómez, P. J., González-Rouco, J. F., Melo-Aguilar, C. & Smerdon, J. E. The role of internal variability in ITCZ changes over the Last Millennium. *Geophys. Res. Lett.* **49**, e2021GL096487 (2022).
42. Alpert, P., Neeman, B. & Shay-El, Y. Climatological analysis of Mediterranean cyclones using ECMWF data. *Tellus Dyn. Meteorol. Oceanogr.* **42**, 65–77 (1990).
43. Doswell III, C. A., Ramis, C., Romero, R. & Alonso, S. A diagnostic study of three heavy precipitation episodes in the western Mediterranean region. *Weather Forecast.* **13**, 102–124 (1998).
44. Beuscher, S. *et al.* End-member modelling as a tool for climate reconstruction—an Eastern Mediterranean case study. *Plos One* **12**, e0185136 (2017).
45. Hafez, Y. Variability of intertropical convergence zone (ITCZ) and extreme weather events. *Atmos. Model Appl.* 121–122 (2012).
46. Jafari, M. & Lashkari, H. Study of the relationship between the intertropical convergence zone expansion and the precipitation in the southern half of Iran. Atm Sol-Terr Phy 210: 1–13. (2020).
47. Okoola, R. Spatial evolutions of the active convective patterns across the equatorial eastern Africa region during Northern Hemisphere spring season using outgoing longwave radiation records. *Meteorol. Atmos. Phys.* **66**, 51–63 (1998).
48. Fontaine, B., Louvet, S. & Roucou, P. Definition and predictability of an OLR based West African monsoon onset. *Int. J. Climatol.* **28**, 1097–1798 (2008).

49. Gadgil, S. & Guruprasad, A. An objective method for the identification of the intertropical convergence zone. *J. Clim.* **3**, 558–567 (1990).

50. Hersbach, H. *et al.* The ERA5 global reanalysis. *Q. J. R. Meteorol. Soc.* **146**, 1999–2049 (2020).

51. Schneider, D. P., Deser, C., Fasullo, J. & Trenberth, K. E. Climate data guide spurs discovery and understanding. *Eos Trans. Am. Geophys. Union* **94**, 121–122 (2013).

52. Byrne, M. P., Pendergrass, A. G., Rapp, A. D. & Wodzicki, K. R. Response of the intertropical convergence zone to climate change: Location, width, and strength. *Curr. Clim. Change Rep.* **4**, 355–370 (2018).

53. Rodríguez-Puebla, C., Encinas, A. & Sáenz, J. y. Winter precipitation over the Iberian peninsula and its relationship to circulation indices. *Hydrol. Earth Syst. Sci.* **5**, 233–244 (2001).

54. Xoplaki, E., González-Rouco, J., Luterbacher, J. & Wanner, H. Wet season Mediterranean precipitation variability: influence of large-scale dynamics and trends. *Clim. Dyn.* **23**, 63–78 (2004).

55. Knippertz, P. & Wernli, H. A Lagrangian climatology of tropical moisture exports to the Northern Hemispheric extratropics. *J. Clim.* **23**, 987–1003 (2010).

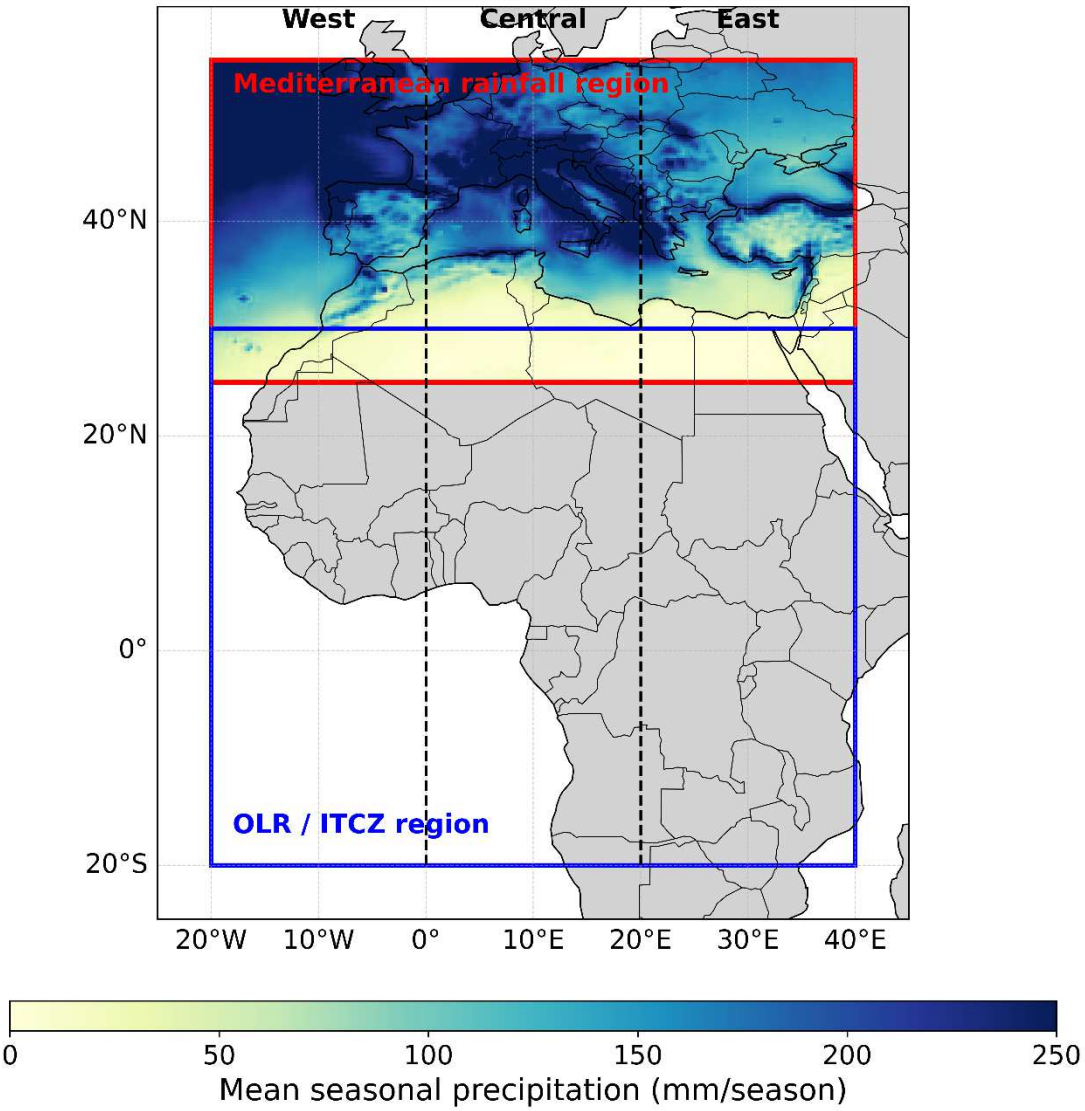
56. Wilks, D. S. *Statistical Methods in the Atmospheric Sciences*. vol. 100 (Academic press, 2011).

57. Vitart, F. *et al.* The subseasonal to seasonal (S2S) prediction project database. *Bull. Am. Meteorol. Soc.* **98**, 163–173 (2017).

58. Waliser, D. E. & Gautier, C. A satellite-derived climatology of the ITCZ. *J. Clim.* **6**, 2162–2174 (1993).

59. Lavers, D. A., Simmons, A., Vamborg, F. & Rodwell, M. J. An evaluation of ERA5 precipitation for climate monitoring. *Q. J. R. Meteorol. Soc.* **148**, 3152–3165 (2022).

630 60. Schwendike, J. *et al*. Local partitioning of the overturning circulation in the tropics
631 and the connection to the Hadley and Walker circulations. *J. Geophys. Res.*
632 *Atmos.* **119**, 1322–1339 (2014).
633 61. Zheng, Y., Meng, Y., Lou, E., Li, Y. & Dong, L. Analysis of global temperature
634 influencing factors based on Spearman correlation coefficient method and grey
635 correlation theory. *Highlights Sci Eng Technol* **48**, 102–111 (2023).
636 62. Hatzaki, M. *et al*. MedCyclones: Working Together toward Understanding
637 Mediterranean Cyclones. *Bull. Am. Meteorol. Soc.* **104**, E480–E487 (2023).
638 63. Lachmy, O. & Kaspi, Y. The role of diabatic heating in Ferrel cell dynamics.
639 *Geophys. Res. Lett.* **47**, e2020GL090619 (2020).
640



641

642 **Figure 1**. Geographical domains used for the analysis of Mediterranean precipitation
643 and ITCZ-related OLR variability, along with the autumn (SON) precipitation
644 climatology (mm season^{-1}) over the Mediterranean study region, averaged over 1940-
645 2024.

646

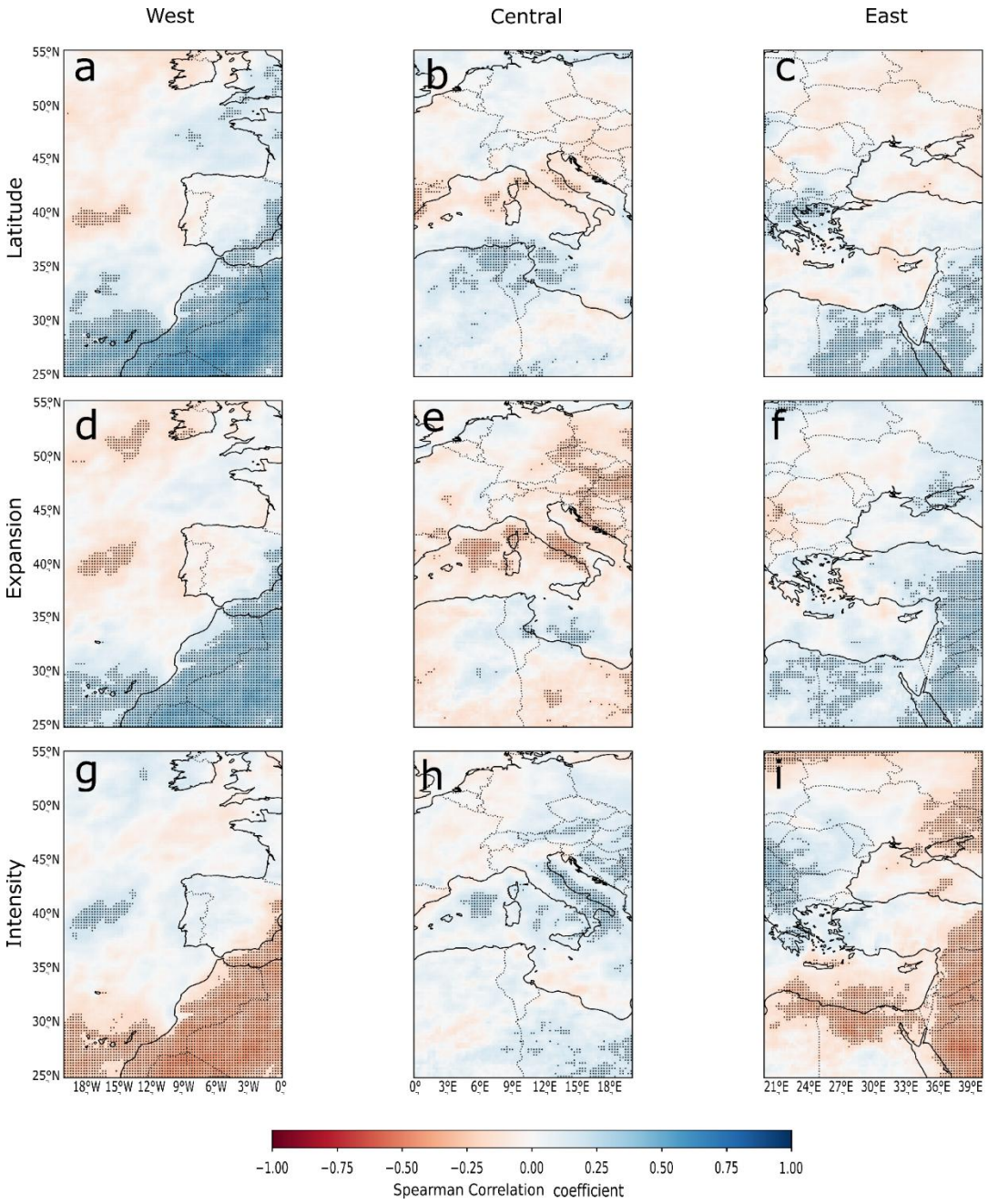
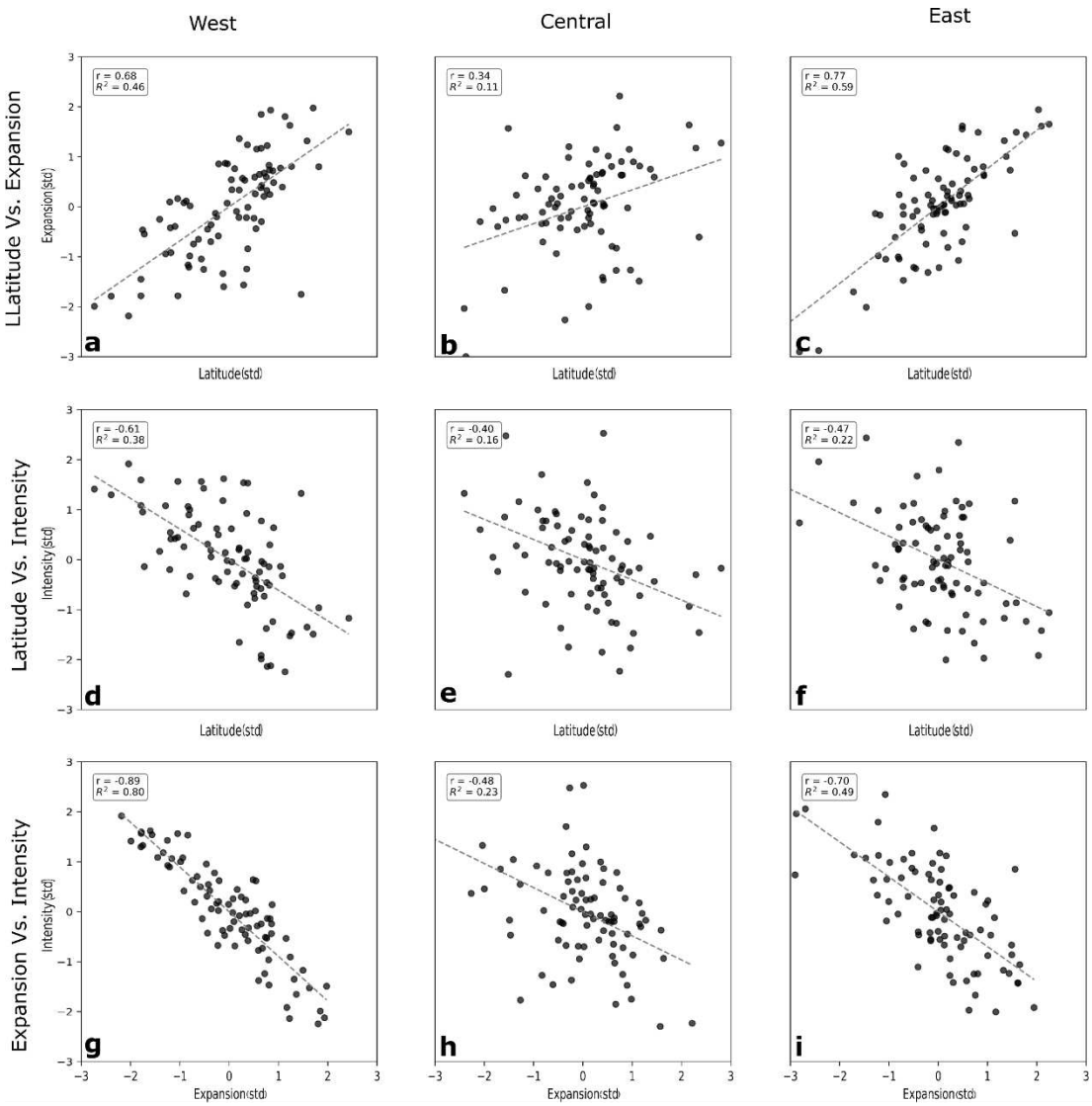


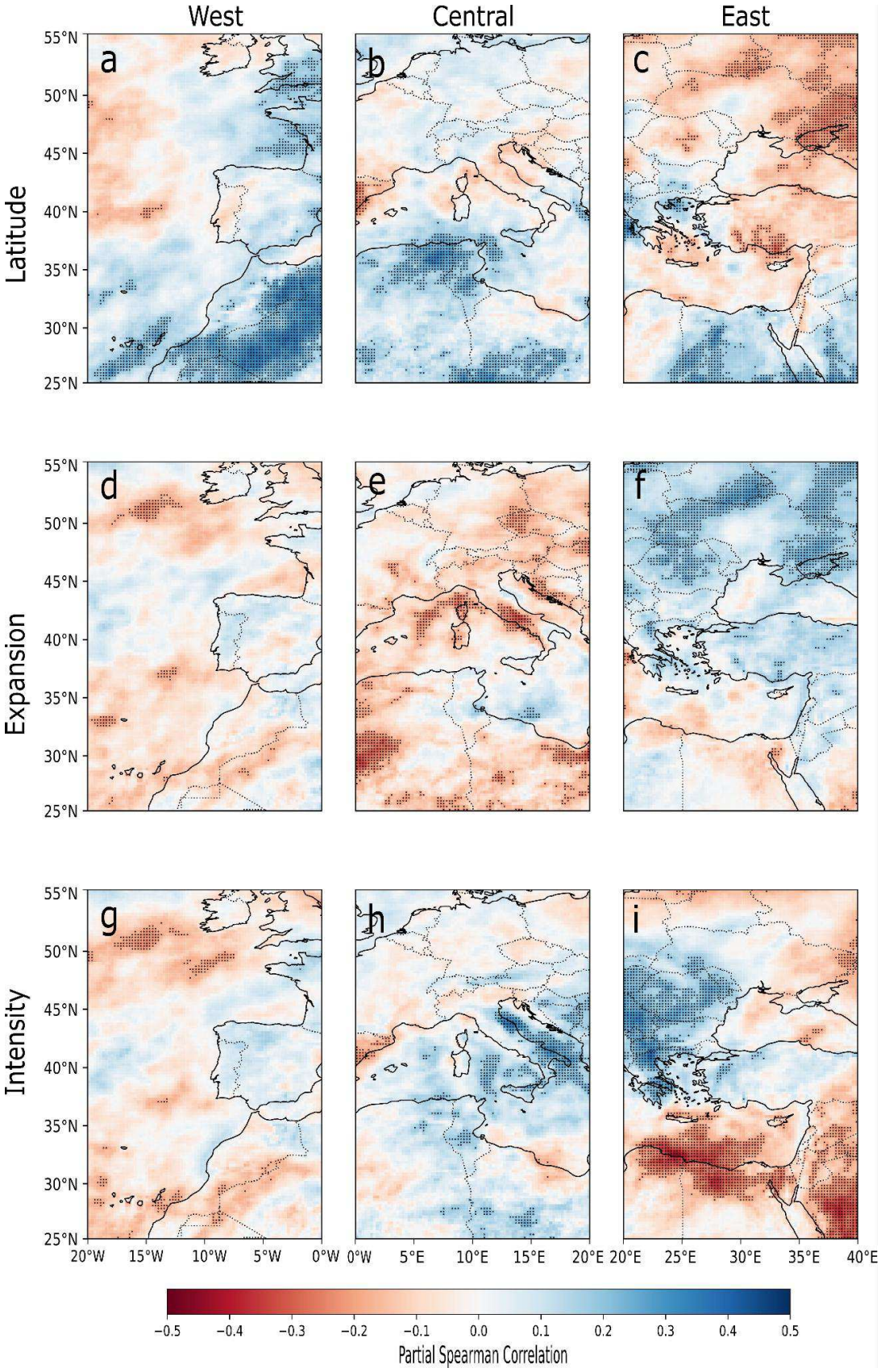
Figure 2 Spearman correlation between autumn (September - November) mean precipitation (ERA5; The exact Figure using the CRU dataset is shown in Fig. S1) and ITCZ category deviations. Columns represent regions (West, Central, East), and rows correspond to ITCZ categories: Latitude (a-c), Expansion (d-f), and Intensity (g-i). Black dots indicate areas where differences are statistically significant at the 90% confidence level, based on a bootstrap test with 1000 realizations.



655 **Figure 3** Scatter plots showing pairwise relationships between standardized ITCZ
656 category deviations (Latitude, Expansion, and Intensity) across the West, Central, and
657 East regions. Each panel shows Pearson correlation coefficients (r) and R^2 values.

658

659



660 **Figure 4** Same as Fig. 1, but it shows the partial correlations of each ITCZ
661 characteristic, controlling for the other two attributes. The exact Figure using the CRU
662 dataset is shown in Fig. S2.

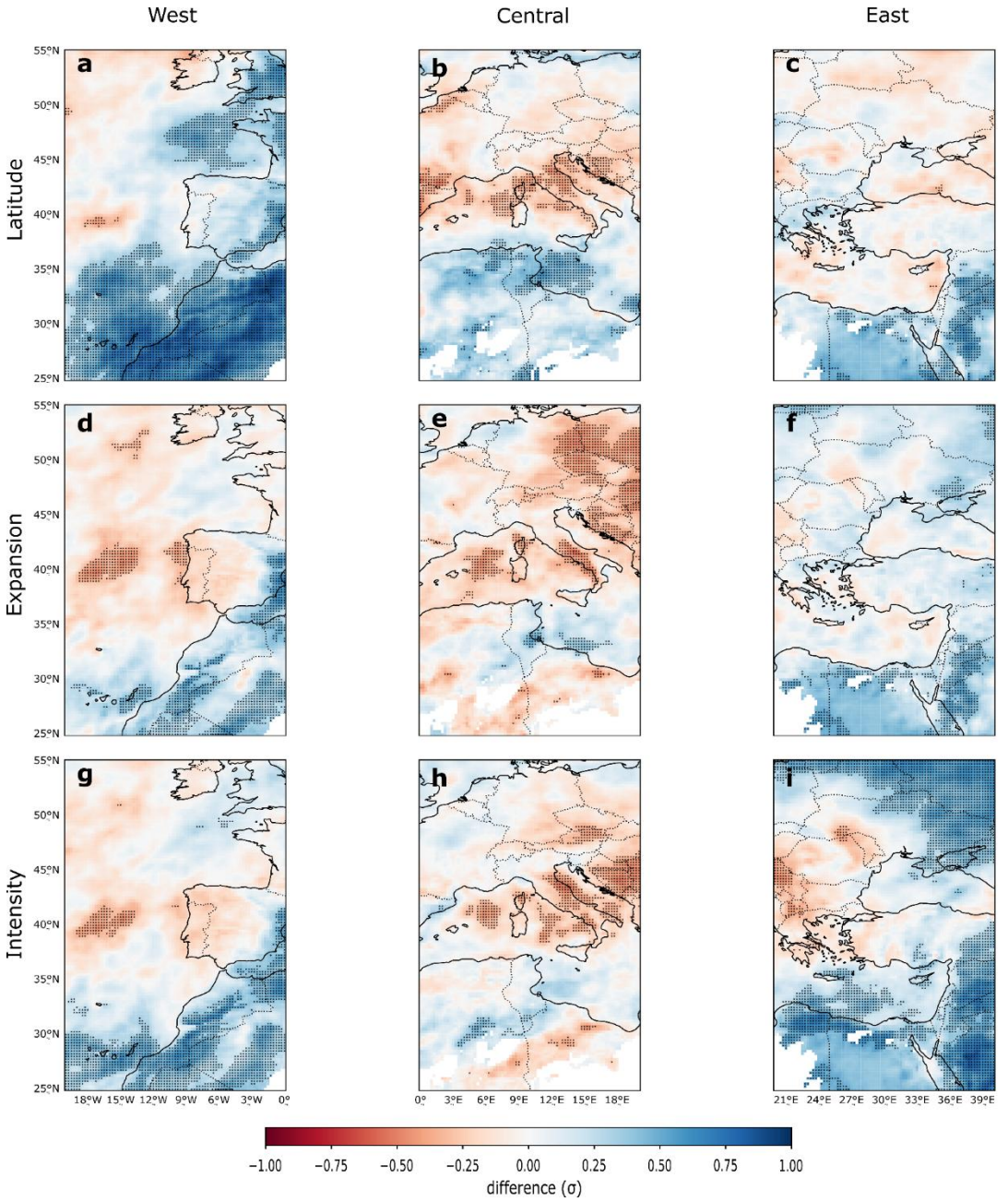
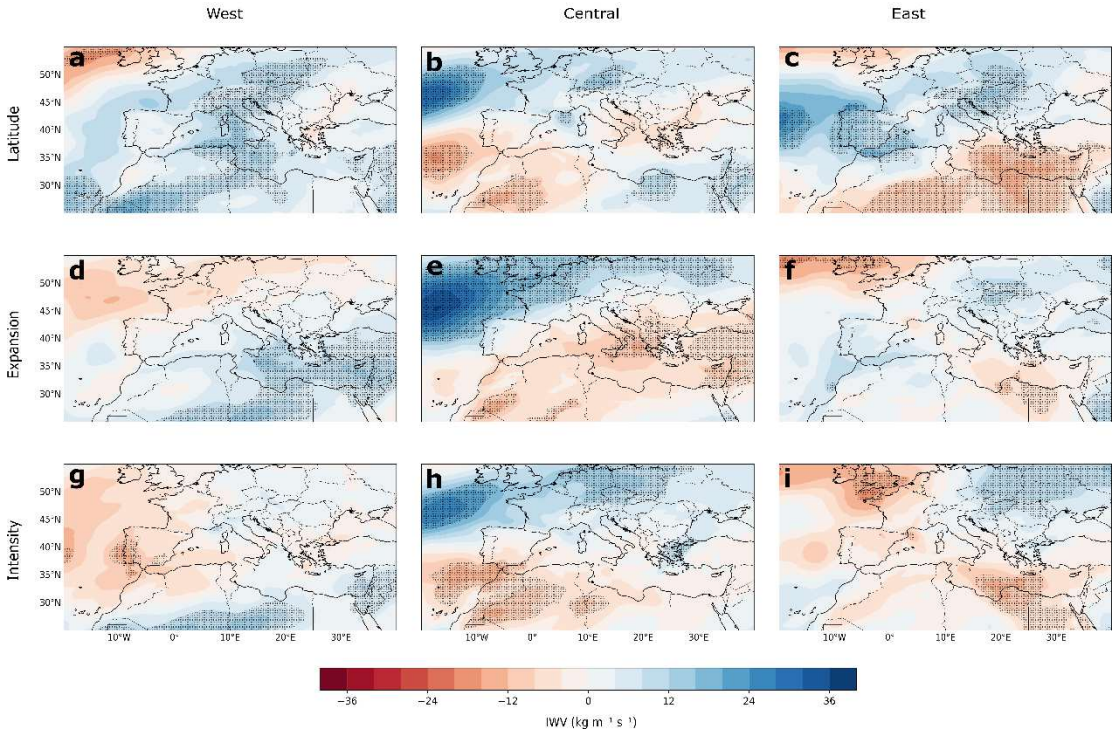


Figure 5 Composite mean differences in standardized precipitation anomalies (ERA5; The exact Figure using the CRU dataset is shown in Fig. S3) between the top and bottom 20% seasons for each ITCZ category. Columns represent regions (West, Central, East), and rows are ITCZ categories: Latitude (a-c), Expansion (d-f), and Intensity (g-i). Black dots indicate areas where differences are statistically significant at the 90% significance level, based on a bootstrap test with 1000 realizations. The typical σ value for North Africa is 0-25 mm season^{-1}, with the northern part of the central and western regions reaching up to 100 mm season^{-1}. Europe's typical σ is 100-150 mm season^{-1}, except in coastal areas, where it reaches 200-250 mm season^{-1}.



673

674 **Figure** 6 Same as Fig. 4, but for the differences in Integrated Water Vapor Transport
675 (IVT).

676

677

678

679

680

681

682

683

684

685

686

687

688

689

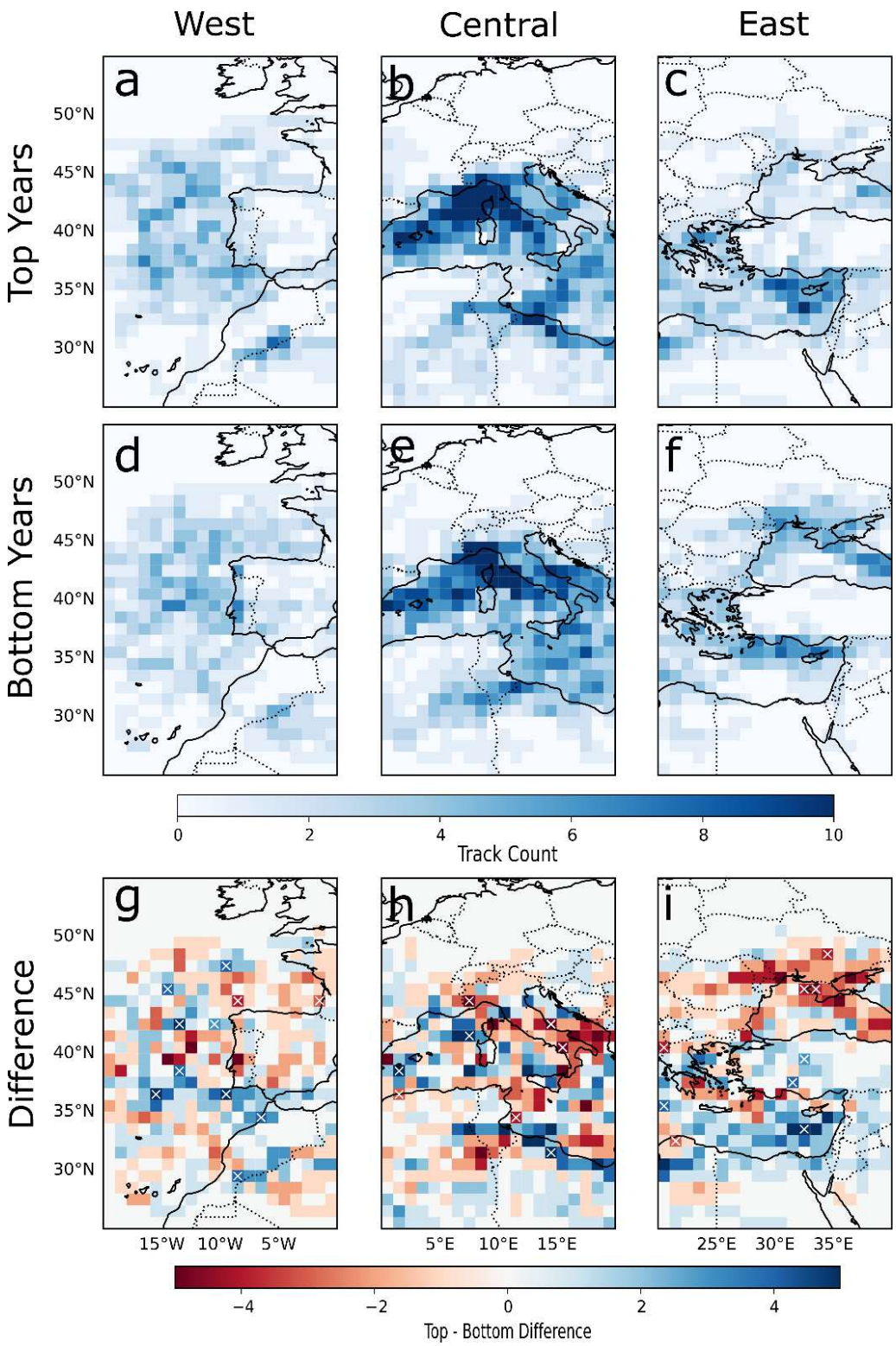
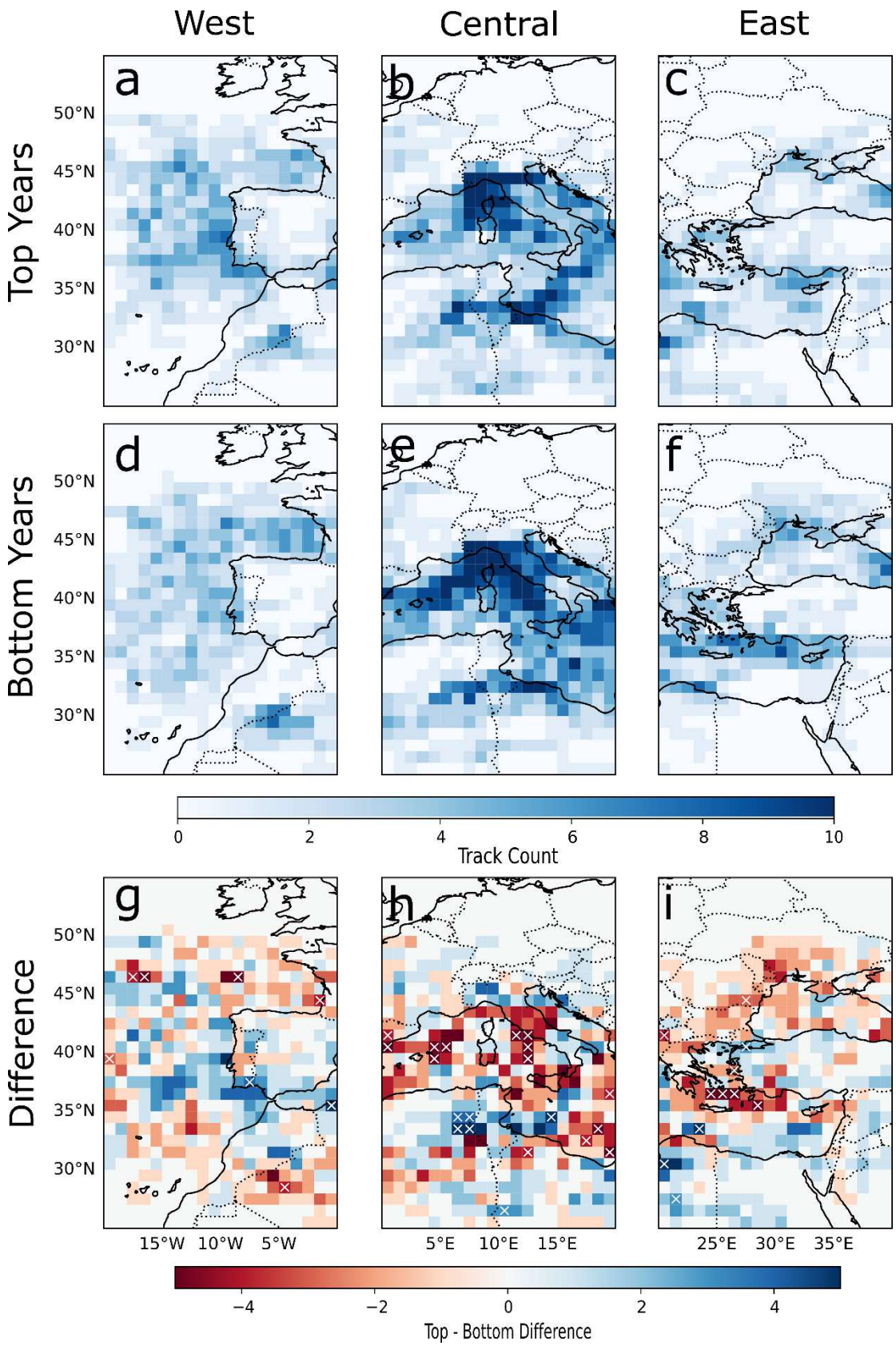


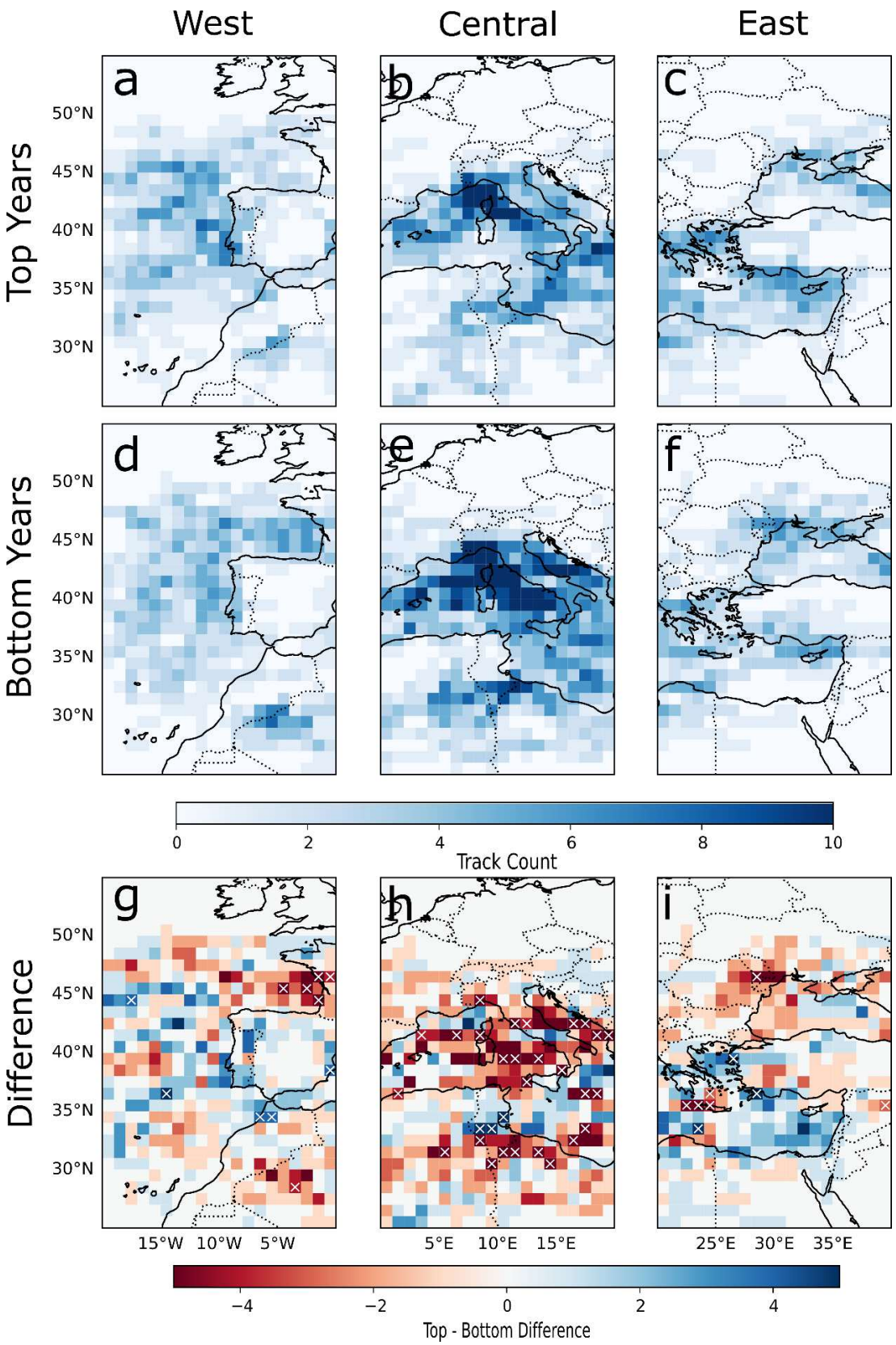
Figure 7 Cyclone track density during the top and bottom 20% of ITCZ latitude seasons for 1979-2020. Columns represent regions (West, Central, East), and rows are: the top 20% of years (a-c), the bottom 20% of years (d-f), and the difference between the top and bottom years (g-i). White × indicates areas where differences are statistically significant at the 90% significance level, based on a bootstrap test with 1000 realizations.



696 **Figure 8** Same as Fig. 6, but for the top and bottom 20% years of ITCZ expansion.

697

698



699 **Figure 9** Same as Fig. 6, but for the top and bottom 20% years of ITCZ intensity.

700

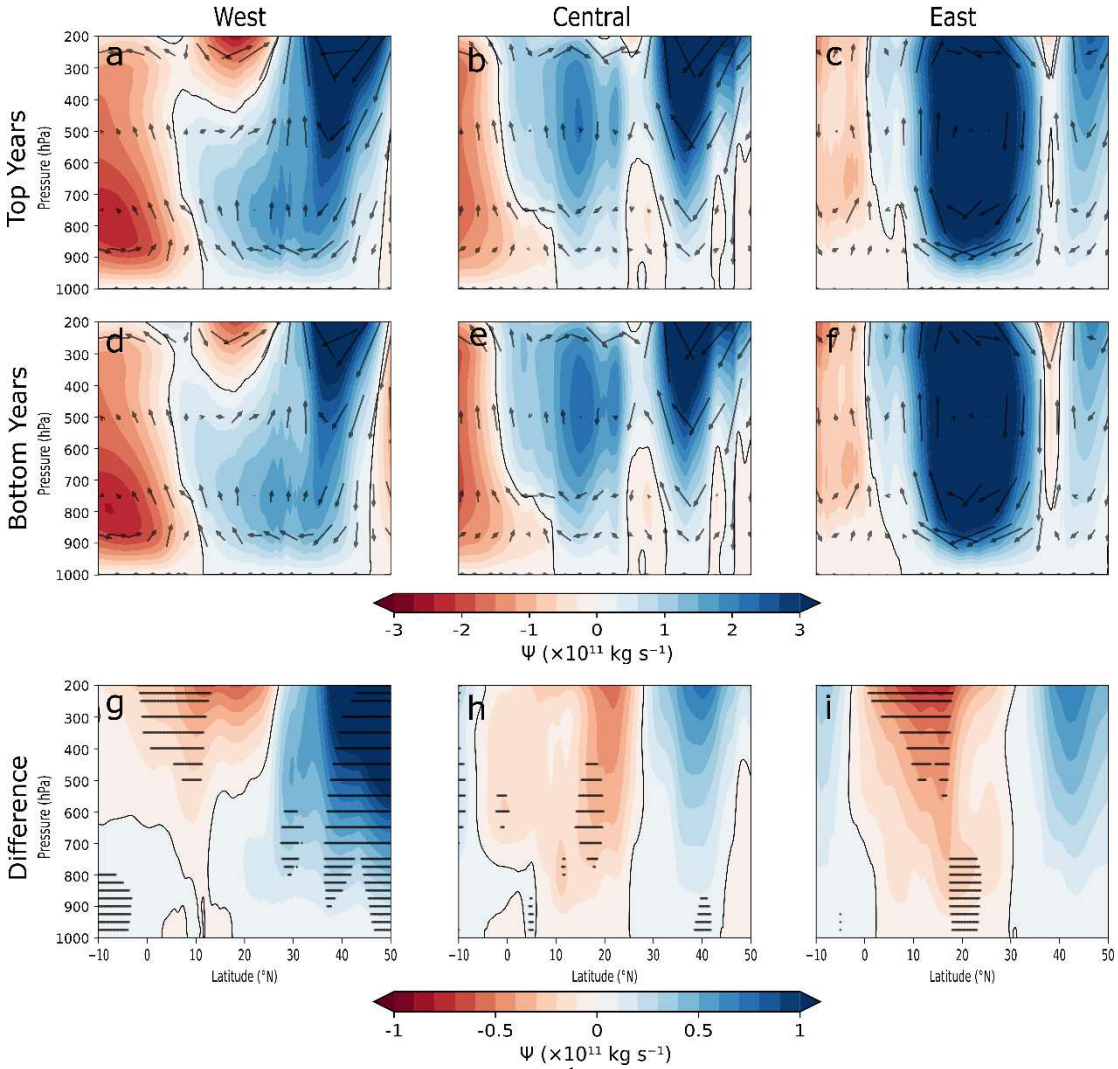


Figure 10 Mass stream function (ψ in kg s^{-1}) during the top and bottom 20% of ITCZ latitude seasons for 1979-2020. Columns represent regions (West, Central, East), and rows are: the top 20% of years (a-c), the bottom 20% of years (d-f), and the difference between the top and bottom years (g-i). Black lines indicate areas where differences are statistically significant at the 90% significance level, based on a bootstrap test with 1000 realizations.

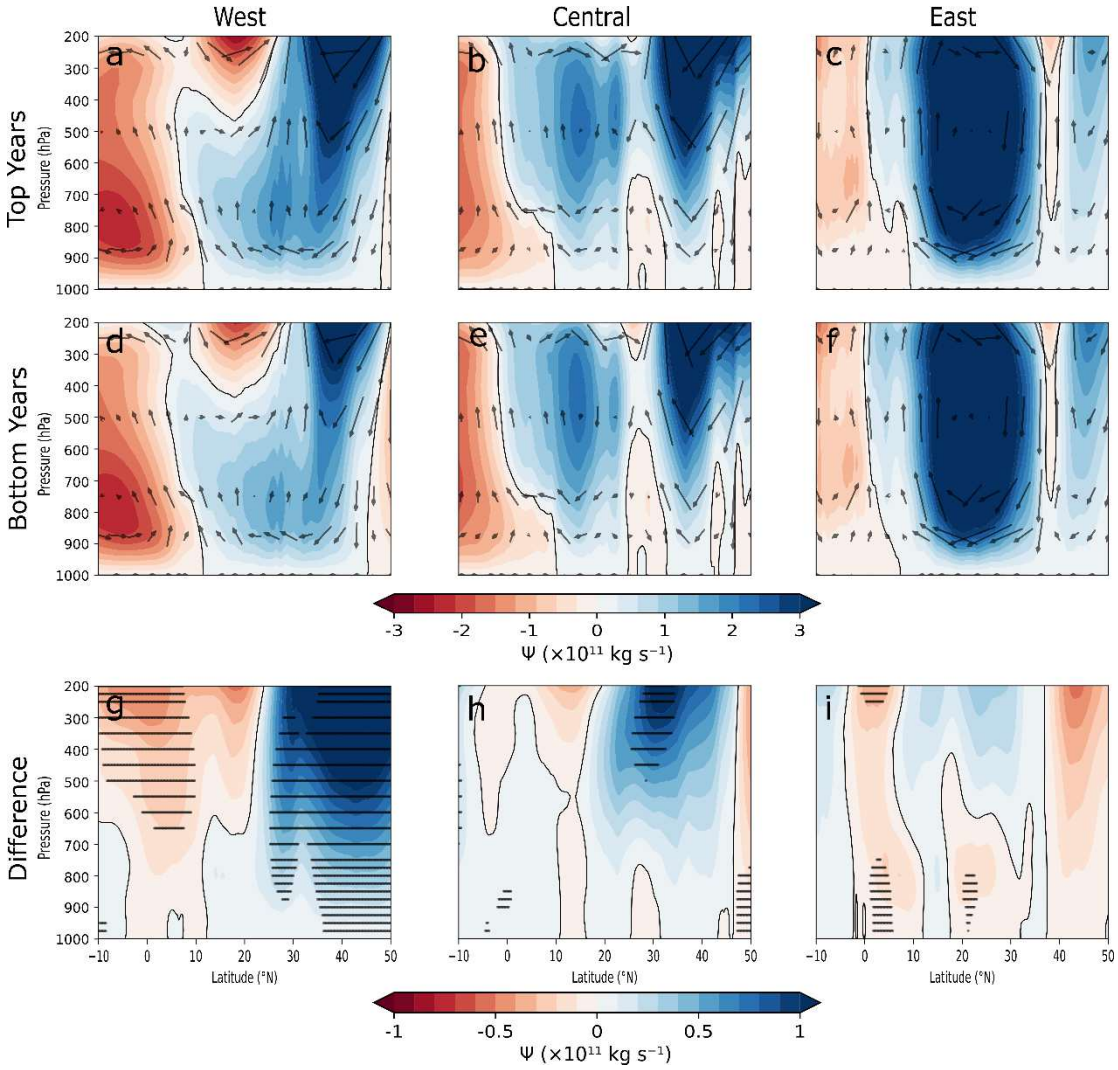
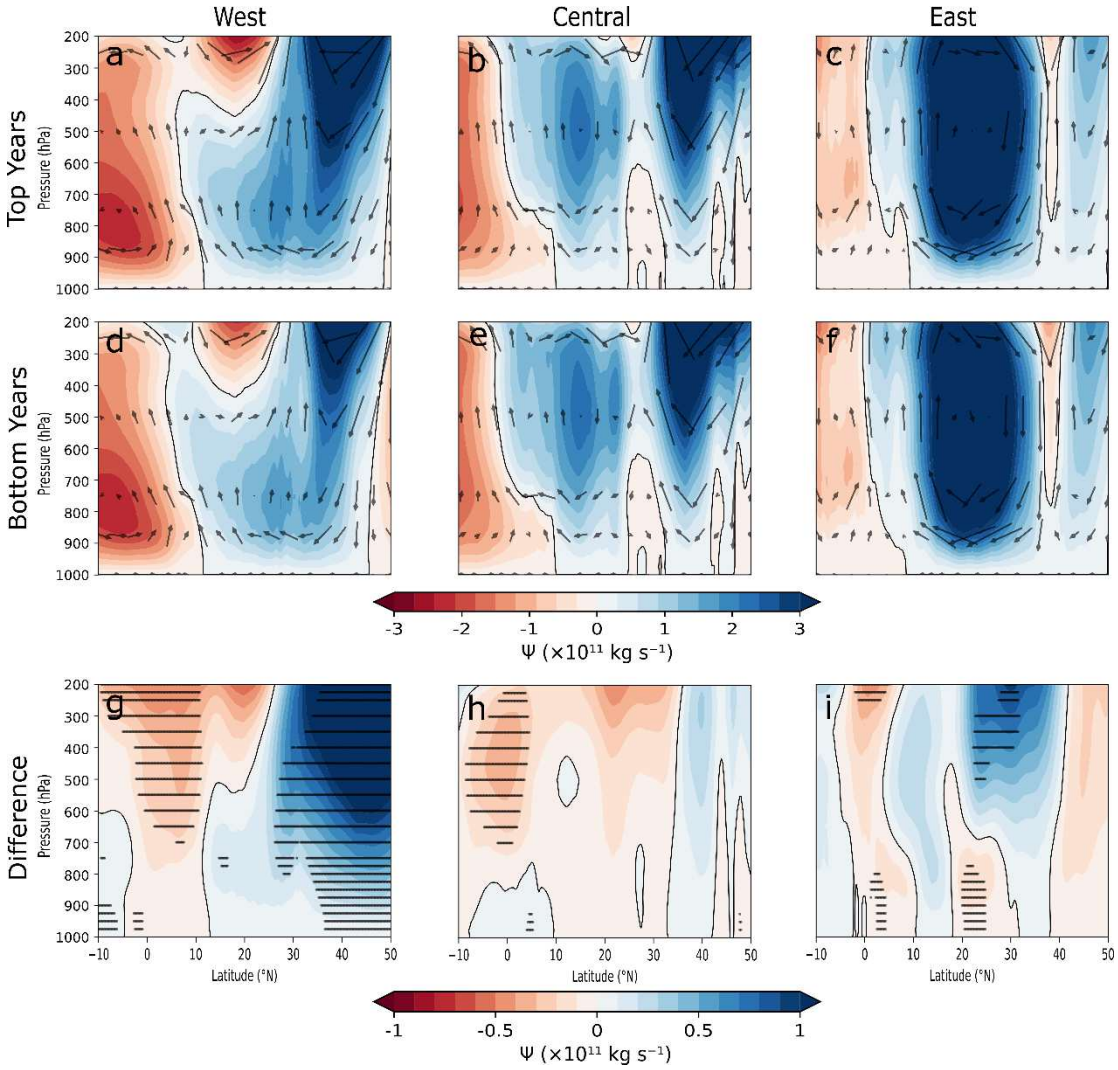


Figure 11 Same as Fig. 9, but for the top and bottom 20% years of ITCZ expansion.



710

711 **Figure 12** Same as Fig. 9, but for the top and bottom 20% years of ITCZ intensity.

712

713

714

715

716

717

718

719

720

721

ITCZ Characteristic	Western Mediterranean	Central Mediterranean	Eastern Mediterranean	Dominant Mechanisms
Latitude (Northward shift)	↑ Precipitation	± Weak response	↑ Precipitation	Enhanced poleward moisture transport across North Africa; strengthened Hadley ascent (25–35° N); increased cyclone density in the east
Expansion (Wider convective zone)	↑ Precipitation (North Africa, Iberia)	± Neutral to ↑	↑ Precipitation (Levant, Balkans)	Broadened tropical moisture pathways; increased integrated water vapor transport (IVT) into the basin; strengthened synoptic activity across southern Europe
Intensity (Stronger convection)	↓ Precipitation	↓ Precipitation	↓ Precipitation, ↑ in southern Europe	Enhanced subtropical subsidence; stabilized lower troposphere; reduced cyclone frequency and moisture transport
Common responses	↑ Moisture flux and ascent under northward/expanded ITCZ	The transitional zone between opposite signals	↑ Cyclone activity and rainfall in northward/expanded phases	Meridional linking between ITCZ convection, Hadley-cell adjustments, and Mediterranean storm track
Hydroclimatic implication	Moisture gateway region - highly sensitive to tropical variability	Transition belt with variable sign and low predictability	Tropical - extratropical bridge - rainfall modulated by ITCZ shifts and local cyclones	ITCZ acts as a dynamic regulator of Mediterranean autumn rainfall via meridional circulation and moisture pathways, not zonal flow changes

722 **Table 1** A summary of the dominant regional mechanisms linking ITCZ variability to
723 Mediterranean hydroclimate. Arrows indicate the direction of precipitation anomalies
724 (↑ increase, ↓ decrease, ± weak or mixed signal).
725
726
727
728

Supplementary Files

This is a list of supplementary files associated with this preprint. Click to download.

- table1.emf
- supportinginformation.docx